Volume 51 | Number 62 | 11 August 2015 | Pages 12335–12506

ChemComm

Chemical Communications

www.rsc.org/chemcomm

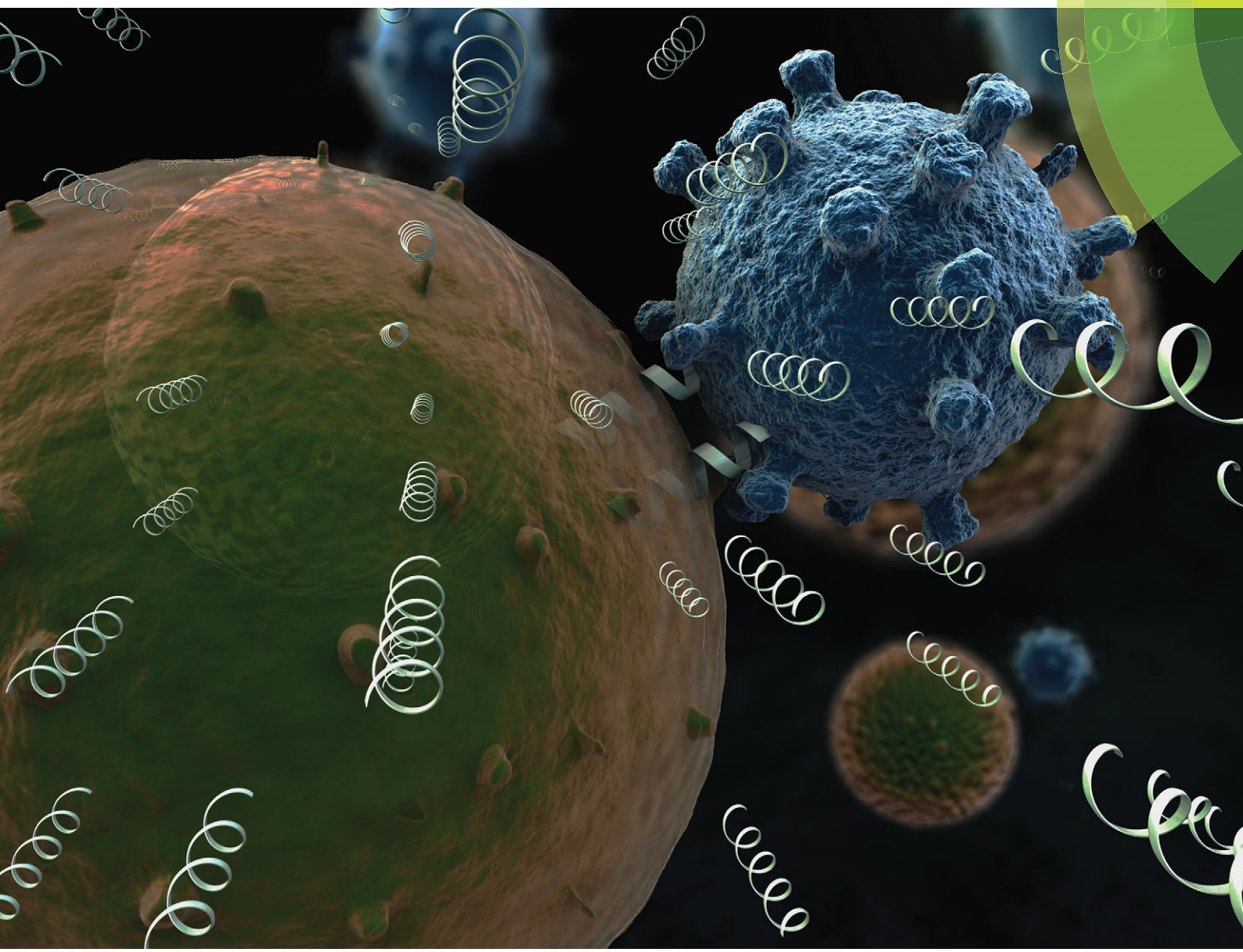

ISSN 1359-7345

ROYAL SOCIETY OF CHEMISTRY

COMMUNICATION

Ehud Gazit *et al.*

α-Aminoisobutyric acid incorporation induces cell permeability and antiviral activity of HIV-1 major homology region fragments

ChemComm

COMMUNICATION

View Article Online
View Journal | View Issue

Cite this: *Chem. Commun.*, 2015, **51**, 12349

Received 15th February 2015,
Accepted 18th June 2015

DOI: 10.1039/c5cc01421b

www.rsc.org/chemcomm

α-Aminoisobutyric acid incorporation induces cell permeability and antiviral activity of HIV-1 major homology region fragments†

Ayala Lampel,[a] Efrat Elis,[b] Tom Guterman,[a] Sharon Shapira,[a] Pini Marco,[c] Eran Bacharach[b] and Ehud Gazit*[ad]

The design of a cell penetrating antiviral peptide, which is derived from the major homology region of HIV-1 capsid protein and includes the non-coded α-aminoisobutyric acid, provides functional evidence for the role of the conserved region in the HIV assembly process and demonstrates the correlation between conformational stability and cellular permeability.

Molecular self-assembly of protein building blocks into ordered supramolecular structures is a key event in major physiological and pathological processes.[1] Virus formation is an important self-assembly event with major clinical outcomes, which is mediated by specific molecular recognition between viral structural proteins to form an intact functional particle.[2] Theoretical modeling and experimental evidence indicate that even a moderate interference with these intermolecular interactions is sufficient to misdirect the assembly pathway of the virus, frequently leading to deformed and non-infectious particles.[3]

The human immunodeficiency virus-1 (HIV-1) first assembles into immature non-infectious assemblies by Gag polyprotein. Later in the virus life cycle, Gag is cleaved by the viral protease, leading to a major structural rearrangement in which a cleavage product of Gag, capsid protein, self-assembles into a capsid structure within the mature and infectious particle.[4] Due to its central role in HIV-1 organization, a number of peptides and small molecules assembly inhibitors of capsid protein were developed.[5] In contrast to the extensive structural characterization of the capsid protein, limited structural information is available on the assembly of Gag within the shell of the immature viral assemblies. The C-terminal domain of the capsid protein (capsid CTD) plays a crucial role in Gag–Gag interactions.[6] This domain contains the most conserved segment in Gag polyprotein which is otherwise highly variable, known as the major homology region (MHR).[7] Mutations in this conserved stretch result in severe defects in the assembly of both the immature and mature viral particles and abolish infectivity.[6,8] Furthermore, a recent cryo-tomography study by Briggs and colleagues implies that MHR residues participate in Gag–Gag interactions.[9] However, these interactions are different from those indicated in a previous model of retroviral immature particles.[10] Hence, further elucidation of the role of the MHR in the assembly process of the immature particle is much needed.

Recently, we determined by X-ray crystallography a new capsid–capsid interface which is mediated in part by four conserved residues located within the MHR: Arg154, Pro157, Lys158 and Arg167 (Fig. 1b).[11] This work provided the first structural evidence for the involvement of the MHR in intermolecular interactions. We suggested that the newly identified capsid–capsid interface may represent an assembly intermediate in the organization of the immature virus and thus can serve as an antiviral target.

Here, we designed a peptide which is derived from the MHR sequence and spans the four conserved residues which interact at the recently reported capsid CTD interface (Pep-V, Fig. 1a and c). Isolated MHR is mainly unfolded in aqueous solutions and an MHR-derived peptide (residues 153–172) was reported to adopt a helical conformation only in the presence of 2,2,2-trifluoroethanol (TFE).[12] In addition, a MHR fragment covering residues 158–176 has been previously reported to inhibit the *in vitro* assembly of capsid protein, but failed to penetrate cells and to efficiently inhibit viral infectivity even when conjugated to a cell penetrating peptide.[13] Thus, to increase the propensity of the designed peptide to adopt a native-like helical conformation, Val165, which does not interact at the capsid–capsid interface, was substituted with the non-coded α-aminoisobutyric acid (Aib) residue (Pep-Aib, compared to Pep-V, Fig. 1a and c). Aib has a pronounced tendency to nucleate α-helical or 3_{10}-helix conformations, even in short peptides[14] due to the restricted geometry imposed by the two methyl groups of the Cα atom, and is used by microorganisms to induce helical conformation in very short peptides.[15]

[a] *Department of Molecular Microbiology and Biotechnology, George S. Wise Faculty of Life Sciences, Tel Aviv University, Tel Aviv 69978, Israel*
[b] *Department of Cell Research and Immunology, George S. Wise Faculty of Life Sciences, Tel Aviv University, Tel Aviv 69978, Israel*
[c] *Department of Molecular Biology & Ecology of Plants, George S. Wise Faculty of Life Sciences, Tel Aviv University, Tel Aviv 69978, Israel*
[d] *Department of Materials Science and Engineering, Iby & Aladar Fleischman Faculty of Engineering, Tel Aviv University, Tel Aviv 69978, Israel*

† Electronic supplementary information (ESI) available. See DOI: 10.1039/c5cc01421b

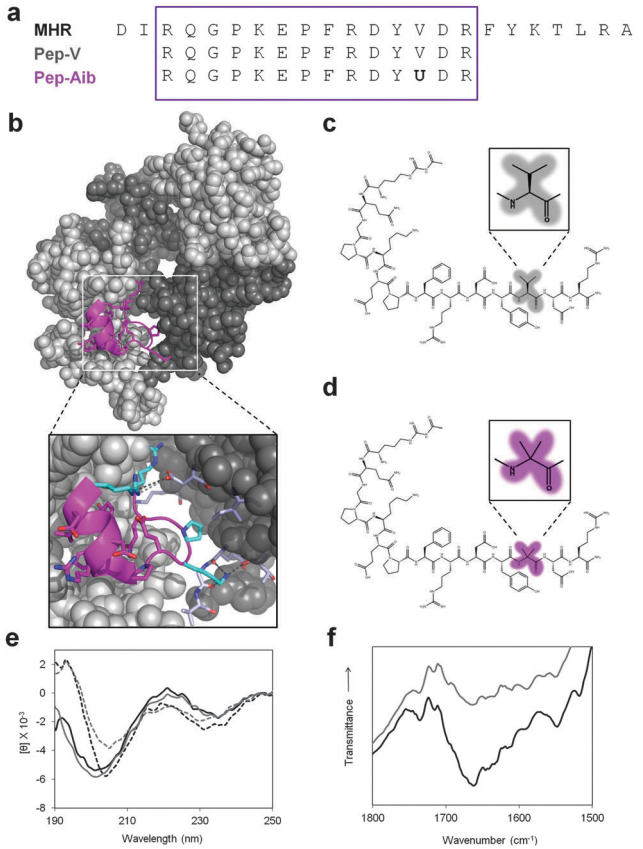

Fig. 1 (a) Sequences of the HIV-1 major homology region (GenBank accession number NP_579880), Pep-V and Pep-Aib. (b) Crystallographic structure of the HIV-1 capsid C-terminal domain tetramer (Protein Data Bank code: 4IPY). MHR fragment is shown as cartoon (magenta) and all side chains are shown as sticks. Enlarged view of the interface: side chains of the interacting interface-residues (cyan), side chains of interacting residues across the interface (light-blue), hydrogen-bonding network (dark grey, dashed) and ionic interaction (light grey, dashed). Chemical structures of Pep-V (c) and Pep-Aib (d) highlighting the Val (grey, enlarged) or Aib (magenta, enlarged) residues, respectively. (e) CD spectra of Pep-V (grey) and Pep-Aib (black) incubated either in the absence (solid lines) or presence (dashed lines) of liposomes and 40% TFE. [θ] = mean residue ellipticity. (f) FTIR spectra showing the amide I region of Pep-V (grey) and Pep-Aib (black).

The conformational state of the peptides was first analyzed by circular dichroism (CD) spectroscopy. When incubated with 0.0125 mg ml^{-1} of liposomes (Experimental section) and 40% TFE in a buffered solution (50 mM sodium phosphate, pH 8.0), the spectra of the peptides showed a positive maximum at 195 nm and a weak negative maximum at 205 nm (Fig. 1e), two features that are strong characteristics of the 3_{10}-helical conformation.[16] In addition, a weak minimum at 230 nm was observed for both peptides. Although this minimum was previously reported for 3_{10}-helical structures of short peptides containing Aib,[16a] here this minimum was also observed for the non-Aib peptide, Pep-V, indicating that the peptide adopts a similar conformation. The key difference between the two spectra was the increased intensity of the minimum at 205 nm in the case of Pep-Aib, suggesting that Pep-Aib has a higher propensity to adopt a characteristic 3_{10}-helical structure. We further analyzed the secondary structure of the peptides by Fourier transform infrared (FTIR) spectroscopy. Both spectra revealed a peak at approximately 1663 cm^{-1} in the amide I region (Fig. 1f), attributed to the 3_{10}-helix conformation.[17] Yet, as observed in the CD spectra, the peak intensity for Pep-Aib was higher than that observed for Pep-V. Taken together, these spectroscopic analyses suggest that both peptides adopt a 3_{10}-helix conformation under the investigated conditions, yet the propensity to adopt this conformation is higher in the case of Pep-Aib as compared to Pep-V.

Next, we examined the ability of the peptides to penetrate mammalian cells, a fundamental requirement for virus assembly inhibitors. For this examination, the peptides were labeled with rhodamine B at the N-terminus. Human embryonic kidney (HEK) 293T cells were treated with each peptide (5 μM) and analyzed using live-cell imaging confocal microscopy. While Pep-V was slightly visible inside the cells, Pep-Aib was highly visible throughout the cytoplasm and nucleus of the cells (Fig. 2a). Quantitative analysis by confocal microscopy demonstrated significantly higher intracellular fluorescence signals in cells treated with Pep-Aib as compared to those treated with Pep-V for 30 min, 1 h and 2 h of incubation (Fig. 2b). Notably, the amino acid sequence of the peptides conforms to a sphingolipid-binding consensus sequence (K/H/R)–X_{1-4}–(Y/F)–X_{4-5}–(K/H/R), where at least one of the X_{1-4} residues is G or T, which may explain the ability of the peptides to penetrate the cells.[18] This consensus sequence was first identified in the V3 loop of the HIV-1 envelope protein gp120[19] and later was also found in various amyloidogenic proteins including prion protein, β-amyloid and α-synuclein.[18,20] The enhanced cell permeability of Pep-Aib compared to Pep-V cannot be attributed to higher hydrophobicity

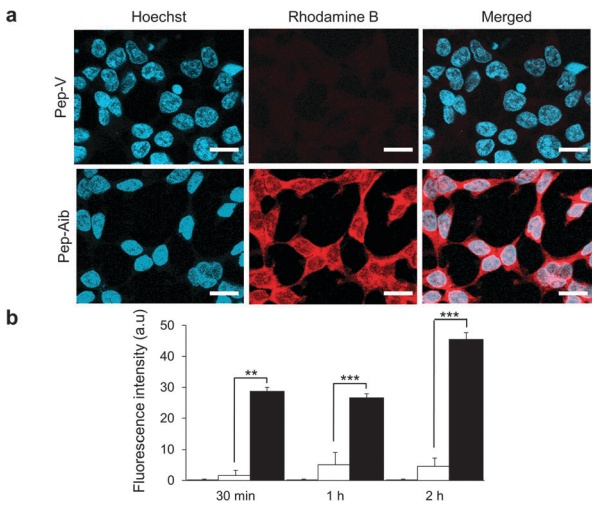

Fig. 2 Cellular uptake of Pep-V and Pep-Aib. (a) Live-cell imaging using confocal fluorescence microscopy of HEK 293T cells treated with 5 μM of rhodamine B-labeled Pep-V (upper panel) or Pep-Aib (lower panel) for 2 h and, after which the nuclei were stained with Hoechst. Scale bars are 20 μm. (b) Quantitative analysis of live-cell confocal microscopy imaging of the peptide cellular uptake. HEK 293T cells were incubated either in the absence (grey) or presence of rhodamine B-labeled Pep-V (white) or Pep-Aib (black) for 30 min, 1 h or 2 h. Values are means ± SD, student's *t*-test, $^{**}p < 0.01$, $^{***}p < 0.001$.

of Pep-Aib, since valine is more hydrophobic than Aib.[21] Therefore and in light of the spectroscopic analyses, we suggest that the improved cell penetration capability of Pep-Aib compared to Pep-V stems from the difference in the conformational state of the peptides. Indeed, previous studies have demonstrated the correlation between cell permeability and high helical propensity of Aib-containing short peptides.[22]

We examined the interaction between the peptides and the structural domain of HIV-1, capsid protein, using fluorescence anisotropy. Changes in the fluorescence anisotropy of dansyl-labeled Pep-V and Pep-Aib were monitored upon the addition of increasing concentrations of purified recombinant HIV-1 capsid protein. As shown in Fig. S1 (ESI†), the presence of capsid protein induced an increase in the fluorescence anisotropy of dansyl-Pep-Aib. Fitting of the binding data indicated that Pep-Aib interacts with capsid protein with an apparent K_D of approximately 7 μM. In contrast, addition of capsid protein to Pep-V yielded no increase in anisotropy, indicative of no binding interaction between this peptide and the protein.

To evaluate the effect of the peptides on viral infectivity, 293T cells were co-transfected with plasmids encoding for vesicular stomatitis virus envelope glycoprotein (VSV-G), HIV-1 Gag and Pol proteins (pCMVΔR8.2) and a retroviral vector encoding for green fluorescent protein (GFP, pHR′CMV-GFP) (Experimental section). 5 h post-transfection, cells were treated with varying concentrations of either peptide. Supernatants containing virus-like particles (VLPs) were collected 48 h post-transfection and were used to infect naïve 293T cells. Infection levels were quantified 48 h post-infection by measuring the reporter GFP^+ cells, using fluorescence-activated cell sorting (FACS). While Pep-V did not affect viral infectivity at any concentration, Pep-Aib decreased the infectivity by more than 40% at 1 μM and 5 μM concentrations and by 66% and 72% at 10 μM and 20 μM concentrations, respectively (Fig. 3a).

The direct effect of the peptides on cell viability was assessed by 2,3-bis-(2-methoxy-4-nitro-5-sulfophenyl)-2*H*-tetrazolium-5-carboxanilide (XTT) assay. The peptides were found to be non-toxic towards 293T cells at concentrations of up to 10 μM. However, both peptides mildly decreased cell viability (10%) at 20 μM (Fig. 3b).

Next, we explored whether Pep-Aib inhibits viral infectivity by interfering with viral assembly. For this purpose, we purified virions which were produced by 293T cells incubated either in the absence or presence of Pep-Aib, using ultracentrifugation through a 25% sucrose cushion. Gag and capsid protein levels inside these virions were analyzed by Western blot assay using an antibody against HIV-1 capsid protein, as a direct measure for virus production. This analysis revealed that Pep-Aib decreased both Gag and capsid levels, suggesting that the peptide reduces extracellular virion levels (Fig. 3c). This finding, together with densitometry quantification revealed that Pep-Aib did not affect intracellular Gag levels (Fig. 3c and d). When Pep-Aib was compared to the previously reported HIV-1 capsid assembly inhibitor CAP-1,[23] the latter compound showed higher inhibition of virus production (Fig. 3c). However, CAP-1, but not Pep-Aib, inhibition was accompanied by high cytotoxicity, as was evident from cell detachment, clamping and highly reduced intracellular actin levels (data not provided).

Next, we performed transmission electron microscopy (TEM) analysis of virions produced in the absence or presence of Pep-Aib to further inspect its effect on the abundance and morphology of the virions. The capsids of mature virions generally appear as central conical structures. Most of the virions which were produced by untreated cells had native-like morphology, with a distinct central cone-shaped density (Fig. 4, 0 μM). In contrast, incubation with Pep-Aib resulted in a low abundance of virions, which presented major morphological defects including twisted and amorphous shapes as well as ruptures (Fig. 4, 1–20 μM). While only 30% of the virions generally have an immature morphology, characterized by the lack of central electron density as reflected by electron microscopy, the predominant morphology of virions which were produced in the presence of Pep-Aib was the immature phenotype (Fig. 4, 1–20 μM). The findings from the anisotropy, infectivity assay, Western blot and TEM analyses imply that Pep-Aib hinders the assembly of either Gag or capsid, leading to a clear decline in virus production and to the formation of aberrant particles with significantly reduced infectivity. Moreover, these findings support recent structural data indicating that contacts between MHR residues stabilize

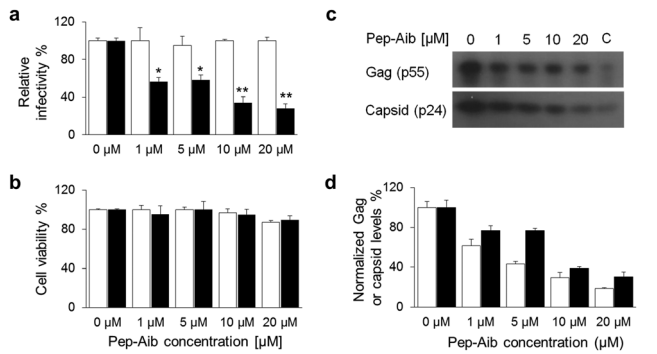

Fig. 3 (a) FACS analysis of Pep-V (white) and Pep-Aib (black) antiviral activity. The relative infectivity is the percentage of infectivity for peptide-treated samples, compared to untreated samples. Bars and error bars represent mean and SD, respectively; n = 3, student's t-test, $*p < 0.05$, $**p < 0.01$. (b) Effect of Pep-V (white) and Pep-Aib (black) on the viability of 293T cells determined using XTT-based cell proliferation assay. Bars and error bars represent mean and SD, respectively; n = 3. (c) Effect of Pep-V, Pep-Aib or CAP-1 (C, 20 μM) on Gag and capsid protein levels analyzed by Western blot using an anti-capsid antibody. (d) Densitometry quantification of Western blot Gag (white) or capsid (black) protein levels.

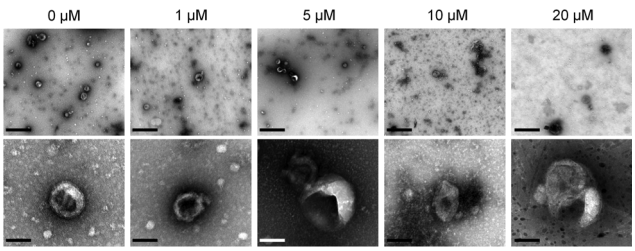

Fig. 4 TEM micrographs of the viral particles produced by 293T cells treated with the indicated concentrations of Pep-Aib. Scale bars of the upper and lower panels are 0.5 μm and 100 nm, respectively.

the hexameric building blocks formed by capsid proteins within Gag during the assembly of the immature particle.[9] We suggest that the Pep-Aib peptide, which is a modified MHR fragment, interferes with early capsid–capsid interactions during the assembly of the immature particle.

To affirm the relation between peptide conformation and its function in cell permeability and antiviral activity, we designed an additional peptide with increased propensity to adopt a helical conformation. The designed peptide contained two Aib residues in positions i and $i + 4$, substituting Pro160 and Tyr164 with Aib, while maintaining the sphingolipid-binding consensus sequence (Aib2, Fig. S2a, ESI†). The CD spectrum of Aib2 with 70% TFE, compared to the spectra of Pep-V, Pep-Aib and a control peptide containing a single Aib substitution at Tyr164 (Aib1), showed a red-shift of the minimum at 205 nm to 207 nm and a blue-shift of the minimum at 230 or 235 nm to 228 nm. In addition, Aib2 exhibited twofold and fivefold increase in the intensity of the positive maximum at 192 nm compared to Aib1 and Pep-V, respectively (Fig. S2b, ESI†). This indicates a higher propensity of Aib2 to adopt a helical conformation compared to the other peptides. Quantitative analysis of live-cell confocal microscopy imaging revealed that cells treated with Aib2 had 50-fold and 150-fold higher fluorescence signal than that of cells treated with Aib1 and Pep-V, respectively (Fig. S2c, ESI†). Finally, Aib2 inhibited 50% of viral infectivity, while Aib1 inhibited ~40% and Pep-V reduced the infectivity by less than 5% (Fig. S2d, ESI†). These results strengthen the relationship between the propensity to adopt a helical conformation, cell penetration capability and the antiviral activity of the designed peptides.

The present study serves as a proof of concept for the design of antiviral agents based on a recently identified capsid–capsid recognition and interaction motif. The inhibitory effect of the MHR-derived peptide on virus assembly provides direct functional evidence that supports recent structural evidence,[9,11] as well as previous genetic information signifying the role of the MHR in the organization of the immature virus.[6] Moreover, our findings support the notion that domain swapping between a dimeric capsid CTD with a deletion mutation, mediated by MHR residues, serves as an assembly intermediate in immature virus formation.[24] Furthermore, the incorporation of the helix inducer non-coded Aib amino acid into the MHR fragment yielded conformational stabilization of the peptide which gave rise to a remarkable increase in the cellular permeability, leading to significant antiviral activity. This demonstrates the incorporation of Aib into synthetic peptides as a simple, yet highly effective, approach in therapeutics-directed molecular engineering. While cellular uptake properties of peptides were previously suggested to be determined mainly by side-chain hydrophobicity,[25] the findings presented here rather emphasize the correlation between conformational stability and cell penetration propensity.

Taken together, our findings illustrate the role of the MHR in HIV-1 assembly and demonstrate the ability to use crystallographic packing data for targeting molecular self-assembly by engineered modules as a means to provide novel directions for antiviral therapy.

This work was supported in part by grants from the Israeli National Nanotechnology Initiative and Helmsley Charitable Trust for a focal technology area on Nanomedicines for Personalized Theranostics. We are grateful to D. Peer for the liposomes, to M. Ehrlich and A. Barbul for the confocal microscopy analysis, to O. Sagi-Assif for FACS analysis and to L. Burlaka (Bar-Ilan University) for TEM analysis. We also thank I. Levinzon and S. Perov for the assistance with CD measurements and to members of the Gazit laboratory for helpful discussions.

Notes and references

1 G. Whitesides, J. Mathias and C. Seto, *Science*, 1991, **254**, 1312.
2 M. J. van Raaij, A. Mitraki, G. Lavigne and S. Cusack, *Nature*, 1999, **401**, 935.
3 P. E. Prevelige, Jr., *J. Mol. Biol.*, 2011, **410**, 634.
4 H. G. Gottlinger, *AIDS*, 2001, **15**, S13.
5 R. Domenech and J. L. Neira, *Curr. Protein Pept. Sci.*, 2013, **14**, 658.
6 (*a*) U. K. von Schwedler, K. M. Stray, J. E. Garrus and W. I. Sundquist, *J. Virol.*, 2003, **77**, 5439; (*b*) B. K. Ganser-Pornillos, U. K. von Schwedler, K. M. Stray, C. Aiken and W. I. Sundquist, *J. Virol.*, 2004, **78**, 2545.
7 J. W. Wills and R. C. Craven, *AIDS*, 1991, **5**, 639.
8 A. Borsetti, A. Ohagen and H. G. Gottlinger, *J. Virol.*, 1998, **72**, 9313.
9 F. K. Schur, W. J. Hagen, M. Rumlová, T. Ruml, B. Müller, H.-G. Kräusslich and J. A. G. Briggs, *Nature*, 2015, **517**, 505.
10 T. A. M. Bharat, N. E. Davey, P. Ulbrich, J. D. Riches, A. De Marco, M. Rumlova, C. Sachse, T. Ruml and J. A. G. Briggs, *Nature*, 2012, **487**, 385.
11 A. Lampel, O. Yaniv, O. Berger, E. Bacharach, E. Gazit and F. Frolow, *Acta Crystallogr., Sect. F: Struct. Biol. Cryst. Commun.*, 2013, **69**, 602.
12 (*a*) C. B. Clish, D. H. Peyton and E. Barklis, *FEBS Lett.*, 1996, **378**, 43; (*b*) R. Domenech, R. Bocanegra, A. Velazquez-Campoy and J. L. Neira, *Biochim. Biophys. Acta*, 2011, **1814**, 1269.
13 R. Bocanegra, M. Nevot, R. Doménech, I. López, O. Abián, A. Rodríguez-Huete, C. N. Cavasotto, A. Velázquez-Campoy, J. Gómez and M. Á. Martínez, *PLoS One*, 2011, **6**, e23877.
14 (*a*) R. Banerjee and G. Basu, *ChemBioChem*, 2002, **3**, 1263; (*b*) K. Basuroy, B. Dinesh, N. Shamala and P. Balaram, *Angew. Chem.*, 2012, **124**, 8866.
15 J. Venkatraman, S. C. Shankaramma and P. Balaram, *Chem. Rev.*, 2001, **101**, 3131.
16 (*a*) S. Tumminakatti, D. N. Reddy and E. N. Prabhakaran, *J. Pept. Sci.*, 2015, **104**, 21; (*b*) N. Berova, P. L. Polavarapu, K. Nakanishi and R. W. Woody, *Comprehensive chiroptical spectroscopy*, John Wiley & Sons, 2012, vol. 2.
17 J. Kong and S. Yu, *Acta Biochim. Biophys. Sin.*, 2007, **39**, 549.
18 J. Fantini and N. Yahi, *J. Mol. Biol.*, 2011, **408**, 654.
19 O. Delezay, D. Hammache, J. Fantini and N. Yahi, *Biochemistry*, 1996, **35**, 15663.
20 (*a*) R. Mahfoud, N. Garmy, M. Maresca, N. Yahi, A. Puigserver and J. Fantini, *J. Biol. Chem.*, 2002, **277**, 11292; (*b*) N. Yahi, A. Aulas and J. Fantini, *PLoS One*, 2010, **5**, e9079.
21 I. Zelezetsky, S. Pacor, U. Pag, N. Papo, Y. Shai, H. G. Sahl and A. Tossi, *Biochem. J.*, 2005, **390**, 177.
22 (*a*) H. Yamashita, Y. Demizu, T. Shoda, Y. Sato, M. Oba, M. Tanaka and M. Kurihara, *Bioorg. Med. Chem.*, 2014, **22**, 2403; (*b*) S.-i. Wada, H. Tsuda, T. Okada and H. Urata, *Bioorg. Med. Chem. Lett.*, 2011, **21**, 5688; (*c*) S.-i. Wada, Y. Hashimoto, Y. Kawai, K. Miyata, H. Tsuda, O. Nakagawa and H. Urata, *Bioorg. Med. Chem.*, 2013, **21**, 7669.
23 C. Tang, E. Loeliger, I. Kinde, S. Kyere, K. Mayo, E. Barklis, Y. Sun, M. Huang and M. F. Summers, *J. Mol. Biol.*, 2003, **327**, 1013.
24 D. Ivanov, O. V. Tsodikov, J. Kasanov, T. Ellenberger, G. Wagner and T. Collins, *Proc. Natl. Acad. Sci. U. S. A.*, 2007, **104**, 4353.
25 J. Farrera-Sinfreu, E. Giralt, S. Castel, F. Albericio and M. Royo, *J. Am. Chem. Soc.*, 2005, **127**, 9459.

